The Relationship between Carotid Arterial Flow and the Left Ventricular Area is valid to indicate contractility in states of cerebral autoregulation and decreased arterial pressure

J Broscheit, F Weidemann, B Grein, M Lange, R Muellenbach, F Schuster, A Koca, C Lintner, E Kunze, J Brederlau, N Roewer, P Steendijk, C Greim

Citation

J Broscheit, F Weidemann, B Grein, M Lange, R Muellenbach, F Schuster, A Koca, C Lintner, E Kunze, J Brederlau, N Roewer, P Steendijk, C Greim. *The Relationship between Carotid Arterial Flow and the Left Ventricular Area is valid to indicate contractility in states of cerebral autoregulation and decreased arterial pressure*. The Internet Journal of Anesthesiology. 2007 Volume 18 Number 2.

Abstract

Background: Myocardial contractility can be estimated by noninvasive ultrasound-derived time-varying elastance ($E\square_{es}$). The $E´_{es}$ is composed of flow in the internal carotid artery located close to the middle cerebral arteries where autoregulated cerebral flow can be accurately detected. Furthermore most contractility indices are highly dependent on ventricular load. We therefore investigated whether the index $E\square_{es}$ is influenced by cerebral autoregulation actuated by decreased arterial pressure which equals also a significant decrease in ventricular load.
Methods: Time-varying elastance was measured in nine merino sheep using a conductance/micromanometer technique to reveal the standard index E_{es}, and by the arterial blood-flow velocity–LV area relationship, resulting in the tested index $E\square_{es}$. The precision to indicate changes in contractility was estimated by the derived indices $\square_{Ees}$ and $\square_{E\square es}$.
Cerebral microcirculation, systolic myocardial dyssynchrony, tissue oxygen of the brain cortex ($p_{(ti)}O_2$) and cerebral cell damage (L/P ratio) were documented. Following a period of stability, mean arterial pressure (MAP) was decreased to 50 mmHg either by the vasodilator sodium nitroprusside (SNP) or by impaired contractility performed with the cardio selective beta-blocker esmolol.

Results: $E´_{es}$ indicated precisely the unchanged myocardial contractility following SNP administration. The index $E\square_{es}$ was valid to detect the decrease in contractility induced by esmolol whereas the precision decreased due to an increase in systolic dyssynchrony.
Conclusions: Our results suggest that autoregulation of cerebral microperfusion and variations in arterial load will not alter $E\square_{es}$ measurements. $E\square_{es}$ is a suitable measurement to use when diagnosing causes of severe hypotension and selecting the appropriate therapy.

INTRODUCTION

In this study, we estimated the range of the ultrasound based index E'_{es} in estimating left ventricular (LV) contractility by measuring E'_{es} in cases of arterial hypotension. [1,2] The arterial hypotension indicates a decrease in LV afterload which severely alters contractility measurements except the standard index E_{es}. In organ tissues arterial hypotension may lead to shock, a potentially life-threatening condition leading to hypoxia of the tissues and consecutively to cell damage [3]. A variety of mechanisms are automatically activated to avoid this fatal outcome. The cerebral autoregulation is an important and well described response of the cerebral arterioles to vary the intraluminary diameter by activating smooth muscles to keep flow constant in cases of pressure variations. A gold standard for the assessment of cerebral autoregulation is not available and the literature shows a considerable disparity of methods and criteria. (This is understandable since cerebral autoregulation is rather just a concept than a physically measurable entity.)

The most common approach to assess cerebral autoregulation tests the effects of changes in mean arterial blood pressure (MAP) on cerebral blood flow in the middle cerebral arteries. The arteries are located close to the internal carotid artery, and the tested effect is known as pressure autoregulation (Gao). The pressure autoregulation only occurs between certain pressure limits – if the pressure drop is to low autoregulation fails, and perfusion of the tissue is comprised. Practically the lower limit is defined as the point where, as the perfusion pressure drops, the flow drops by a predefined value, commonly at 15% and reliable occurring at values below 45 mmHg. It was previously thought that this flow in the cerebral arteries will be constant throughout the "autoregulatory range", and than drop off at a precise lower threshold. More recent and general work suggests that it is simplistic, and that autoregulation follows interindividual varying curves that near the lower limits of autoregulation (Gao). If the lower limit once is exceeded the organ perfusion is comprised consecutively leading to cell damage and organ dysfunction. Thus an adequate monitoring of sufficient tissue perfusion is essential for testing the hypothesis. The testing of pressure autoregulation requires acute blood pressure-lowering which is broadly performed intravenously by the potent peripheral vasodilator sodium nitroprusside (SNP) (Circulation 2004, Immink, van den Born, van Montfrans, Koopmans, Karemaker, van Lieshout).

The hypothesis of the present investigation is that the index E'_{es}, estimating contractility by the relationship of blood flow velocity in the internal carotid artery and area of the left ventricular cavity is not comprised by cerebral autoregulation and furthermore by decreased arterial pressure indicating an increase in afterload. We therefore decreased MAP down to 50mmHg by the use of SNP. Since in the operating room it is common to lower MAP down to hypotensive values, e.g. during microscopic surgery to decrease bleeding by applying beta-blocking agents, we also expanded our protocol by lowering MAP with the cardioselective beta-blocker esmolol.

MATERIALS AND METHODS

In one case we could not analyse the metabolites because of a defect microcatheter. Nine Merino sheep (mean age 2 ± 0.2 y; mean weight 63 ± 4 kg) were used for this study. The study protocol was approved by the Committee for Laboratory Animal Care at our university; the protocol also conforms to the guiding principles of the American Heart Association on research animal use [4].

ANESTHESIA

Anesthesia was performed according to our previously published protocol [2], except that intramuscular premedication was performed with 1.5–2.0 mg/kg xylazine hydrochloride (Rompun; Bayer AG, Leverkusen, Germany). Arterial oxygen saturation was monitored by continuous-pulse oximetry at the shaved ear of the sheep, and arterial blood gases were controlled periodically (995-AVL; Medizintechnik GmbH, Bad Homburg, Germany).

PREPARATION

Figure 1 illustrates the placement of the probe, lines, and catheters, and explains which catheters were used to monitor which parameters. Under X-ray guidance a conductance catheter (Zoetermeer, The Netherlands) was placed into the LV cavity, via the left femoral artery, along the long axis to permit continuous measurement of intraventricular pressure and volume. A polyethylene catheter was advanced 15 cm into the descending aorta from the right femoral artery, and another was advanced into the inferior vena cava from the femoral vein. A thermodilution catheter was advanced into the pulmonary artery via the left internal jugular vein to the superior vena cava to measure stroke volume. A Fogarty catheter was advanced into the inferior vena cava from the right femoral vein to achieve temporary rapid preload reduction by inflating the terminal balloon. Via a left-sided thoracotomy, a 5-MHz echoprobe (T6210, Hewlett Packard, Andover, MA) was sutured onto the myocardial wall to acquire the cross-sectional view of the left ventricle. A U-shaped Doppler flow probe was placed around the exposed right carotid artery. A pacemaker was not applied to maintain a constant heart rate during the sequential periods.

After craniotomy, a laser Doppler flowmeter [5] was fixed in the brain cortex to measure relative flux transdurally in the right frontal area. A ti-pO_2 catheter (Licox Systems, GMS Kiel-Mielkendorf, Germany) and a microdialysis-catheter (CMA 70 Microdialysis Brain Catheter, Solna, Sweden) were inserted subcortically in the right frontal area. The ti-pO_2 and microdialysis catheters were fixed at 10 mm subdurally in the white matter of the frontal region. Care was taken to ensure that the distance between both catheters was at least 1 cm. After the surgical procedure of approximately 1.5–2 h, the animals were observed for 60 min to document hemodynamic stability.

Figure 1

Figure 1: Placement of probes, lines, and catheters

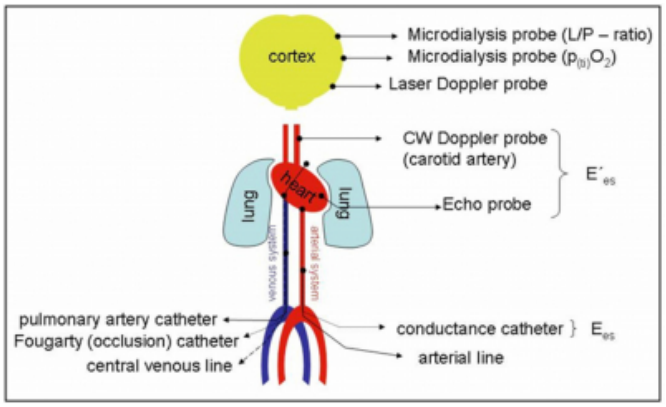

CONDUCTANCE CATHETER

To determine E_{es}, we continuously calculated LV volume from the specific conductivity of the blood [6,7], as well as the offset of the conductivity and fluids surrounding the LV cavity [8]. The contribution of parallel conductance to the total conductance signal was derived from a measurement of the conductance signal during passage of the bolus through the LV. For absolute volume measurements, we determined the slope factor , which was introduced to account for the finding that the relationship between “true” volume and conductance did not fall on the line of identity, even after correcting for parallel conductance [7]. This may result from the fact that equipotential planes are not exactly parallel in the cavity, indicating a nonhomogeneous current distribution. In addition, it may partly result from a mismatch between the electrode distances and the ventricular long axis [9]. There is no simple way to determine ; its value can be estimated by comparing conductance-derived volume with an independent measure, such as changes in cardiac output (CO) following thermodilution [10].

Global contractility of the LV was determined by applying the time-varying elastance model [11]. Time-varying elastance was carried out during rapid preload reduction by occlusion of the inferior vena cava every 7 ms of the cardiac cycle, beginning with the end-diastolic point and continuing past the end-systolic point. Maximal elastance was the elastance connecting the zero point on the coordinate cross with the end-systolic point. Linear regression analysis of the end-systolic values during occlusion of the inferior vena cava by rapid preload reduction was used to obtain the slope of LV E_{es}. The amount of the decrease in LV end-systolic pressure-volume relationship (LVESPV) as a response to the rapid preload reduction depends on the myocardial contractility as expressed by the index E_{es}. The equation for calculating E_{es} is:

Figure 2

$$E_{es} = \frac{\Delta P}{\Delta V}$$

A gently inclined linear curve implies a substantial decrease in LV volume and a concomitant smooth decrease in LV pressure, which characterizes compromised contractility.

MECHANICAL DYSSYNCHRONY

At each time point, a segmental signal was defined as dyssynchronous if its change (i.e., dVseg/dt) was opposite to the simultaneous change in the total LV volume (dVLV/dt). Segmental dyssynchrony is quantified by calculating the percentage of time within the cardiac cycle when a segment is dyssynchronous. Overall LV dyssynchrony (DYS) was calculated as the mean of the segmental dyssynchronies [12]. DYS can be calculated within each specified time interval: we determined DYS during systole (DYSS) and diastole (DYSD), with systole defined as the period between the moments of dP/dtmax and dP/dtmin.

INTERNAL FLOW

Nonuniform contraction and filling is associated with ineffective shifting of blood volume within the LV. This internal flow (IF) is quantified by calculating the sum of the absolute volume changes of all segments and subtracting the absolute total volume change: IF(t) = [|dVseg,i(t)/dt | – | dVLV(t)/dt|]/2. Note that dVLV(t)/dt represents the effective flow into or out of the LV. Thus, IF measures the segment-to-segment blood volume shifts, which do not result in effective filling or ejection. Division by two takes into account that any noneffective segmental volume change is balanced by an equal and opposite volume change in the remaining segments. Systolic IF fraction (IFFS) is calculated by integrating IF(t) over the full cardiac cycle and dividing by the integrated absolute effective flow (28).

BLOOD-FLOW VELOCITY/LV AREA RELATIONSHIP

Continuous ultrasound-mediated estimation of LV volume for determining E'_{es} was performed using an automated detection technique as previously described [1,2]. To obtain the time-varying elastance E'_{es} from the blood-flow velocity-area loops, we used two-dimensional echocardiograms of the LV cavity in short-axis view recorded simultaneously with measurements of blood-flow velocity in the carotid artery, as previously performed [1]. We plotted arterial blood-flow velocity against the corresponding area. The end of systole was defined as the time at which the elastance reached a maximal value, termed E'_{max}, for every loading beat synchronized in time [11]. These points on the end-systolic blood-flow velocity area loops were obtained during rapid LV preload reduction induced by inferior caval vein occlusion. The slope of the regression curve calculated from the end-systolic blood-flow velocity area points was defined as elastance E'_{es} [13]. Analogous to E_{es}, the decrease in LV end-systolic flow-area relationship (LVESFA) as a response to the rapid preload reduction equals the myocardial contractility as expressed by the index E'_{es}. The equation for calculating E'_{es} is:

Figure 3

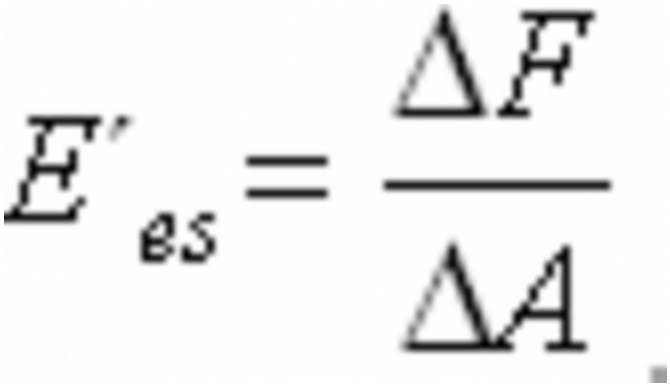

$$E'_{es} = \frac{\Delta F}{\Delta A}$$

Compromised contractility is characterized by a gently inclined slope, which implies a substantial decrease in LV area and a concomitant smooth decrease in LV blood flow velocity.

LASER DOPPLER

We monitored cerebral microcirculation by laser Doppler flowmetry, an established technique for real-time measurement of microvascular red blood cell perfusion in tissue [5]. Perfusion is also referred to as microvascular blood flow or red blood cell flux and is proportional to the product of the average speed of the blood cells and their number concentration (often referred to as blood volume). This value is expressed in arbitrary "perfusion units" and is calculated using the first moment of the power spectral density. Although such measurements are proportional to perfusion, the factor of proportionality varies for different tissues. A calibration of the Doppler-flow measurement using the conductance catheter is not yet available. Therefore, we calculated the relative flux by dividing the flux obtained during the interventions by their corresponding baseline values. The laser Doppler imager recorded cerebral perfusion in the temporal domain and presented the data throughout the experiment. The relative flux served as a record of the cerebral microcirculation, whereas the blood-flow velocity of the carotid artery established the blood-flow velocity-area relationship to calculate E'_{es}.

Cerebral autoregulation is locally heterogeneous due to the anatomical variation of the brain cortex [14,15]. This heterogeneity necessitated a sequential procedure that excluded alternative methods of perfusion measurement, such as the tracer microsphere technique. This technique delivers absolute measures but only allows documentation of the status quo without disturbing microcirculation. Consequently, we excluded relative flux from the multiple testing procedures because all other parameters were absolute values.

CEREBRAL MICRODIALYSIS

Cerebral microdialysis was used to record whether the lower border of cerebral autoregulation was passed. Changes in $p_{(ti)}O_2$ provide the earliest sign of hypoxia/ischemia [16]; the microdialysis assays of metabolism provide additional information about the consequences of reduced tissue $p_{(ti)}O_2$ [17]. Hypoxia occurs below the $p_{(ti)}O_2$ threshold of 15–10 mmHg [17,18]. Baseline levels of the lactate-to-pyruvate ratio (L/P) can vary between 15–22; an increase above 30 indicates cerebral cell damage, as supported by the decrease in $p_{(ti)}O_2$ [19].

We carefully inserted a microdialysis probe (CMA 70 brain microdialysis catheter; 1-cm membrane tip, 0.62-mm diameter; CMA Microdialysis) into the brain tissue next to a $p_{(ti)}O_2$ probe. Perfusion (CMA107 Microdialysis Pump) of the catheter with sterile modified Ringer's solution was started before implantation. The flow rate was 2 μL/min and fractions were collected every 15 min. Online analysis of samples was performed using the CMA 600 microdialysis

analyzer (CMA Microdialysis). Lactate, pyruvate, and $p_{(ti)}O_2$ concentrations were determined using extracellular fluid probes.

To observe the autoregulation pattern, height, and area, we positioned the probe far from large vessels in a relatively avascular region of the cortex; however, the sensitive region measured by the laser Doppler flow probe approaches the 1- to 2-mm spacing in oxygen heterogeneity observed in the normal cat cortex [20]. This distance approached the 300-700 μm spacing between two of Bär's medium vascular nodules [21], and recent work by Lübbers et al. [22] showed oxygen heterogeneity with the same spacing. Several studies support the interpretation that interanimal variations in laser Doppler flow and $p_{(ti)}O_2$ are caused by variations within the cortex of each animal [15,23].

HEMODYNAMIC MEASUREMENTS

We determined all hemodynamic parameters during apnea prior to rapid preload reduction by occlusion on the inferior vena cava.

ESMOLOL AND SNP ADMINISTRATION

Esmolol was used to acutely reduce MAP to 50 mmHg (when compared with the corresponding baseline levels) by impairing myocardial contractility. To exclude influences of cardiac load on E'_{es}, we sequentially induced a similar hypotension in the same animal using the arterial vasodilator SNP. The two hemodynamic stages were induced in random sequence for each sheep; either SNP (4 μg/kg/min) or esmolol (2–5 mg/kg) was infused and held constant for 15 min. Baseline measurements were taken prior to each stage (baselines 1 and 2). SNP decomposes into pharmacologically inactive metabolites within a few minutes of infusion [24]. Esmolol is an ultra short-acting cardioselective beta-antagonist with an extremely short elimination half-life (mean, 9 min; range, 4–16 min) that has a total body clearance [285 ml/min/kg (17.1 L/h/kg)] approaching three times CO and 14 times hepatic blood flow [25]. We waited 60 min after the end of each intervention before initiating the next intervention.

STATISTICAL ANALYSIS

Data are expressed as mean ± standard deviation (SD). Direct comparisons were made using either the Student's t-test or the Mann Whitney U test. Statistical significance was inferred when $p < 0.05$.

The relative changes (Δ) of elastance in both systems (Δ_{Ees} and $\Delta_{E'es}$) that followed each intervention were calculated by the formulae:

eq3

Positive and negative values of Δ_{Ees} indicated an increase or decrease in LV contractility, respectively. The agreement between Δ_{Ees} and $\Delta_{E'es}$ was tested according to Bland and Altman [26]: differences and arithmetic means were plotted and the SD of the differences was calculated.

RESULTS

HEMODYNAMIC MEASUREMENTS

All hemodynamic parameters are shown in Table 1. MAP decreased significantly from the baseline following both SNP (50 ± 11 mmHg) and esmolol (48 ± 6 mmHg) infusions, reaching intended levels. There was no significant difference between the baseline values. Esmolol infusion caused heart rate to decrease significantly (73 ± 14 min^{-1}) as compared with baseline (90 ± 21 min^{-1}) and SNP (94 ± 23 min^{-1}) values. CO decreased significantly as a result of esmolol infusion, as compared with the baseline (2.4 ± 1.0 $ml \cdot min^{-1}$) and following SNP infusion (3.2 ± 2.0 $ml \cdot min^{-1}$).

Figure 4

Table 1: Hemodynamic and microdialysis data.

	Baseline	SNP	Esmolol
MAP [mmHg]	90 ±16	50 ±1#	48 ±6#
E_{es} [mmHg·cm^{-3}]	3.0 ±0.9	3.0 ±0.7	1.0 ±0.2#,+
E'_{es} [cm^{-3}]	0.89 ±0.24	0.76 ±0.27	0.36 ±0.21#,+
ς_{Ees} [%]	1	-11.0 ±11.7	-58 ±17#
$\varsigma_{E'es}$ [%]	1	-11.6 ±12.6	-55 ±16#
IFF_{sys} [%]	15 ±4.8	21 ±15	27 ±9.3#,+
DYS_{sys} [%]	17 ±3.4	18 ±4.5	23 ±5.1#,+
HR [bpm]	90 ±21	94 ±23	73 ±14#,+
CO [l·min^{-1}]	5.2 ±1.6	6.3 ±4.0	3.6 ±0.6#,+
CVP [mmHg]	6 ±2	5 ±2	7 ±2
LVESV [ml]	48 ±8	47 ±10	99 ±25#,+
LVEDV [ml]	123 ±14	122 ±22	114 ±28
EF [%]	50 ±10	46 ±10.8	26 ±7.2#,+
LVESP [mmHg]	100 ±20	54 ±10#	57 ±22#
LVEDP [mmHg]	12 ±6.5	8 ±5.5	10 ±5
Flux [mm·s^{-1}]	1	0.84 ±0.20	0.63 ±0.30#
$p_{(ti)}O_2$ [mmHg]	33 ±23	34 ±7	14 ±13#,+
L/P-ratio [-]	12 ±3	19 ±8	28 ±15#,+

NOTE: Mean ± standard deviation; n = 9.

Abbreviations: CO, cardiac output; DYS_{sys}, LV dyssynchrony during systole; E_{es}, end-systolic elastance; $E'_{e,s}$ end-systolic elastance of the flow velocity-area relationship; EF, ejection fraction; HR, heart rate; IFF_{sys}, LV internal flow fraction during systole; L/P-ratio, ratio of lactate and pyruvate values; LVEDV, LV end-diastolic volume; LVEDP, end-diastolic pressure; LVESV, end-systolic volume; LVESP, end-systolic pressure; MAP, mean arterial pressure; $p_{(ti)}O_2$, partial oxygen pressure in the tissue; SNP, sodium nitroprusside; SW, stroke work; ς_{Ees} – relative change of the elastance E_{es}; ς_{Ees} – relative change of the elastance E'_{es}.

# $p < 0.05$ compared with baseline.

+ $p < 0.05$ compared with SNP.

CONTRACTILITY MEASUREMENTS

The blood-flow velocity-area relationship in a single animal during the sequential pharmacological interventions is displayed in Figure 2. The E_{es} of each relationship indicated a significant decrease in LV contractility attributable to esmolol (1.0 ± 0.2 mmHg·cm $^{-3}$) as compared with baseline (3.0 ± 0.9 mmHg·cm $^{-3}$) and SNP (3.0 ± 0.7 mmHg·cm $^{-3}$) values. The E'_{es} decreased following esmolol infusion (0.36 ± 0.21 sec $^{-1}$ ·cm $^{-1}$) as compared with baseline values (0.88 ± 0.26 sec $^{-1}$ ·cm $^{-}$) and the value following SNP infusion (0.76 ± 0.27 sec $^{-1}$ ·cm $^{-1}$).

Figure 2. Loops of the flow-area and pressure-volume relationship during sequential periods. Pressure-volume and velocity–LV area data from one animal at baseline, during sodium nitroprusside SNP administration, and during esmolol administration. End-systolic points and corresponding slopes are shown, demonstrating increased and decreased end-systolic elastance.

CEREBRAL AUTOREGULATION

The parameter flux acquired by laser Doppler flowmetry is shown in Table 1. The decrease of Flux following SNP infusion was within the range of 15% deviation from baseline and therefore within the limits of autoregulation. The decrease following esmolol was significantly stronger than the decrease following SNP infusion averaging at 37% deviation from baseline values and therefore ranging below cerebral autoregulation.

TISSUE PERFUSION

Cerebral perfusion. The parameters obtained by microdialysis are given in Table 1. In two cases, we could not analyze lactate and pyruvate levels because of a defective microcatheter. The $p_{(ti)}O_2$ was unchanged following SNP infusion and significantly decreased by 50% following esmolol infusion as compared with the baseline and SNP values. L/P reflects the degree of anaerobic glycolysis and indicates the degree of cellular tissue damage due to cerebral hypoxia [27] . According to our predefinition, we would expect an increase in L/P to indicate that the lower limit of autoregulation processes had been passed over which should be the case when 15% of Flux. L/P increased significantly from the baseline following esmolol application, and L/P was significantly higher after esmolol infusion than after SNP infusion.

p(tiO2 vs. L/P. The data pairs from seven animals during the

four sequential periods were sampled for correlations. Of these, 28 data pairs were used for analysis; the results are depicted in Figure 3. The curve fitting revealed evidence of a power function for overall data pairs (Figure 3):

$p_{(ti)}O_2 = 69.3\ LP^{-0.5}$ (1)

with R = 0.82, $R^2 = 0.67$, and $p < 0.0001$. The striking variance revealed by the regression analysis relating $p_{ti}O_2$ and L/P can be attributed to the heterogeneous time delay of the induced metabolic response [18,28].

Figure 5

Figure 3: L/P vs. pO2. Plots of the 28 pooled data pairs demonstrating the relationship of indices derived from the cerebral tissue oxygen and the cerebral metabolites. Results for regression analysis of pO from cerebral tissue oxygen vs. L/P calculated from cerebral metabolites) are shown; = 0.90, = 0.81, and < 0.0001.

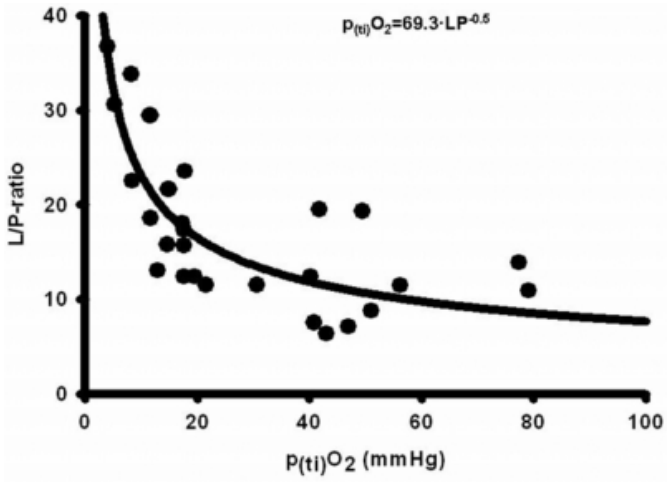

Myocardial perfusion. The parameters indicating mechanical dyssynchrony are supposed to represent myocardial perfusion and summarized in Table 1. The increases in IFFS and DYSS due to SNP infusion were not significant whereas esmolol infusion was followed by a significant increase in IFFS and DYSS.

PRECISION OF E' IN INDICATING CONTRACTILITY

Analysis of the changes in E_{es} and E'_{es} are presented in Table 1. Sharing common units, we forwarded Δ_{Ees} and $\Delta_{E'es}$ to a bias plot as described by Bland-Altman (Figure 4A and 4B).

The effects of altered LV contractility on E'_{es} and E_{es} of the left ventricle are shown in Table 1, and are expressed by the relative contractility changes and . The analysis of the SNP and baseline values to estimate the changes in contractility revealed a systematic bias (mean ± SE) of 0.029 (2.9%) ± 0.064 (6.4%) in estimating E_{es} by E'_{es}. The 95% confidence interval was ± 1.96 SE, which equals 13%. The response to SNP infusion resulted in good agreement between E_{es} and E'_{es}, as indicated by regression analysis, and Bland-Altman analysis demonstrated an acceptable agreement between E_{es} and E'_{es} in indicating contractility changes (Figure 4A).

The bias plot of the esmolol values of the parameters Δ_{Ees} and $\Delta_{E'es}$ used to detect changes in contractility revealed a systematic bias (mean ± SE) in estimating E_{es} by E'_{es} of 0.43 (43%) ± 0.3 (30%). The 95% confidence interval was ± 1.96 SE, which equals 59% (Figure 4B). This is a striking decrease in the agreement of E'_{es} with E_{es}.

Figure 4. Plot of the difference against the mean for relative contractility change (Δ_{Ees} and $\Delta_{E'es}$) data. The thick line represents the mean, and the broken lines indicate ± 2 standard deviations (SD).

(A) Values for SNP vs. baseline before SNP, SNP vs. baseline before esmolol, and baseline before esmolol vs. baseline before SNP.

(B) Values for esmolol vs. baseline before esmolol and esmolol vs. baseline before SNP.

DISCUSSION

The present study was performed to test whether a new, ultrasound-based index E'_{es} can validly quantify LV myocardial contractility in cases of significant arterial hypotension. The acquired data suggests that the index E'_{es} will not be influenced by the autoregulated perfusion flow of the brain. (Autoregulation of the cerebral arteries implies that varying pressure perfusing those arteries is followed by only little changes of the flow through the brain.) The proof of the hypothesis was evident because E'_{es} is composed of the blood-flow velocity in the internal carotid artery close to the middle cerebral arteries where autoregulated blood flow is reliably detected by established clinical tests.

Arterial hypotension indicates a significant reduction in LV afterload. Most of the tests indicating myocardial contractility are highly dependent on the ventricular load and show substantial variations under varying load. We could demonstrate that the index E'_{es} generates valid data during arterial hypotension until cardiac function is maintained.

The present study also demonstrated that LV dyssynchronic contraction appears to be the major cause of decreased

accuracy in the ability of E'_{es} to quantify contractility. Recently, we showed that a dyssysnchronic LV contraction caused by regional ischemia reduces the efficiency of the LV to transpose contractility into an outward flow–directed contraction resulting in an increase of internal flow and in a limited capacity of E'_{es} to quantify contractility (article in press).

For clinical purpose our data underline the necessity to differentiate between impaired contractility and significant volume shift in cases of arterial hypotension. Both states may have a notably different impact on the clinical course. The arterial hypotension due to a volume shift induced no perfusion disturbances. Whereas the same impact on arterial pressure following a decrease in contractility caused reasonable cell damage and cardiac dysfunction. Either way we would emphasize cardiac imaging if the reason of remarkable arterial hypotension tends to be unclear. It should not be unmentioned that impaired contractility and volumeshift require disparate therapeutic consequences.

At this point we want to stress that the analysis of tissue oxygenation in dependence to the acquired hemodynamic data is beyond the scope of tested hypothesis.

In summary, cerebral autoregulation and significant arterial hypotension will not alter E'_{es} measurements up until the occurrence of myocardial ischemia. Therefore, E'_{es} is a valid indicator of myocardial contractility

References

1. Broscheit JA, Greim CA, Kessler M, Weidemann F, Roewer N: Determination of preload-recruitable stroke work and elastance by the relationship of arterial blood flow velocity to left ventricular area. J.Cardiothorac.Vasc.Anesth. 2004; 18: 415-22
2. Broscheit JA, Weidemann F, Strotmann J, Steendijk P, Karle H, Roewer N, Greim CA: Time-varying elastance concept applied to the relation of carotid arterial flow velocity and ventricular area. J.Cardiothorac.Vasc.Anesth. 2006; 20: 340-6
3. Pianim NA, Liu SY, Dubecz S Jr, Klein SR, Bongard FS: Tissue oxygenation in hypovolemic shock. J.Surg.Res. 1993; 55: 338-43
4. Position of the American Heart Association on research animal use. Circulation 1985; 71: 849A-50A
5. Swiontkowski MF, Tepic S, Perren SM, Moor R, Ganz R, Rahn BA: Laser Doppler flowmetry for bone blood flow measurement: correlation with microsphere estimates and evaluation of the effect of intracapsular pressure on femoral head blood flow. J.Orthop.Res. 1986; 4: 362-71
6. Baan J, Jong TT, Kerkhof PL, Moene RJ, van Dijk AD, van der Velde ET, Koops J: Continuous stroke volume and cardiac output from intra-ventricular dimensions obtained with impedance catheter. Cardiovasc.Res. 1981; 15: 328-34
7. Baan J, van der Velde ET, de Bruin HG, Smeenk GJ, Koops J, van Dijk AD, Temmerman D, Senden J, Buis B: Continuous measurement of left ventricular volume in animals and humans by conductance catheter. Circulation 1984; 70: 812-23
8. Steendijk P, Baan J: Comparison of intravenous and pulmonary artery injections of hypertonic saline for the assessment of conductance catheter parallel conductance. Cardiovasc.Res. 2000; 46: 82-9
9. Baan J, Vandervelde ET, Steendijk P: Ventricular Pressure Volume Relations Invivo. European Heart Journal 1992; 13: 2-6
10. Burkhoff D, van d, V, Kass D, Baan J, Maughan WL, Sagawa K: Accuracy of volume measurement by conductance catheter in isolated, ejecting canine hearts. Circulation 1985; 72: 440-7
11. Sagawa K: The end-systolic pressure-volume relation of the ventricle: definition, modifications and clinical use. Circulation 1981; 63: 1223-7
12. Schreuder JJ, Steendijk P, van der Veen FH, Alfieri O, van der NT, Lorusso R, van Dantzig JM, Prenger KB, Baan J, Wellens HJ, Batista RJ: Acute and short-term effects of partial left ventriculectomy in dilated cardiomyopathy: assessment by pressure-volume loops. J.Am.Coll.Cardiol. 2000; 36: 2104-14
13. Sagawa K, Suga H, Shoukas AA, Bakalar KM: End-systolic pressure/volume ratio: a new index of ventricular contractility. Am.J.Cardiol. 1977; 40: 748-53
14. Jones SC, Radinsky CR, Furlan AJ, Chyatte D, Qu YS, Easley KA, Perez-Trepichio AD: Variability in the magnitude of the cerebral blood flow response and the shape of the cerebral blood flow: Pressure autoregulation curve during hypotension in normal rats. Anesthesiology 2002; 97: 488-96
15. Kimme P, Ledin T, Sjoberg F: Cortical blood flow autoregulation revisited using laser Doppler perfusion imaging. Acta Physiol Scand. 2002; 176: 255-62
16. Hlatky R, Valadka AB, Goodman JC, Contant CF, Robertson CS: Patterns of energy substrates during ischemia measured in the brain by microdialysis. J.Neurotrauma 2004; 21: 894-906
17. Valadka AB, Goodman JC, Gopinath SP, Uzura M, Robertson CS: Comparison of brain tissue oxygen tension to microdialysis-based measures of cerebral ischemia in fatally head-injured humans. J.Neurotrauma 1998; 15: 509-19
18. Meixensberger J, Kunze E, Barcsay E, Vaeth A, Roosen K: Clinical cerebral microdialysis: Brain metabolism and brain tissue oxygenation after acute brain injury. Neurological Research 2001; 23: 801-6
19. Reinstrup P, Stahl N, Mellergard P, Uski T, Ungerstedt U, Nordstrom CH: Intracerebral microdialysis in clinical practice: Baseline values for chemical markers during wakefulness, anesthesia, and neurosurgery. Neurosurgery 2000; 47: 701-9
20. Wilson DF, Gomi S, Pastuszko A, Greenberg JH: Microvascular Damage in the Cortex of Cat Brain from Middle Cerebral-Artery Occlusion and Reperfusion. Journal of Applied Physiology 1993; 74: 580-9
21. Bär T: Distribution of radially penetrating arteries and veins in the neocortex of rat, Cerebral Microcirculation and Metabolism.. Edited by Cervós-Navarro J FE. New York, Raven Press, 1981, p pp 1-pp 8
22. Lubbers DW, Baumgartl H: Heterogeneities and profiles of oxygen pressure in brain and kidney as examples of the pO(2) distribution in the living tissue. Kidney International 1997; 51: 372-80
23. Schiszler I, Tomita M, Fukuuchi Y, Tanahashi N, Inoue K: New optical method for analyzing cortical blood flow

heterogeneity in small animals: validation of the method. American Journal of Physiology-Heart and Circulatory Physiology 2000; 279: H1291-H1298
24. Schulz V: Clinical pharmacokinetics of nitroprusside, cyanide, thiosulphate and thiocyanate. Clin.Pharmacokinet. 1984; 9: 239-51
25. Wiest D: Esmolol. A review of its therapeutic efficacy and pharmacokinetic characteristics. Clin.Pharmacokinet. 1995; 28: 190-202
26. Bland JM, Altman DG: Statistical-Methods for Assessing Agreement Between 2 Methods of Clinical Measurement. Lancet 1986; 1: 307-10
27. Willis N, Mogridge J: Indicators of histohypoxia. Acta Anaesthesiol.Scand.Suppl 1995; 107: 45-8
28. Meixensberger J, Vath A, Jaeger M, Kunze E, Dings J, Roosen K: Monitoring of brain tissue oxygenation following severe subarachnoid hemorrhage. Neurological Research 2003; 25: 445-50

Author Information

J. Broscheit
Department of Anesthesiology, University Clinics of Wuerzburg

F. Weidemann
Department of Internal Medicine, University Clinics of Wuerzburg

B. Grein
Department of Anesthesiology, University Clinics of Wuerzburg

M. Lange
Department of Anesthesiology, University Clinics of Wuerzburg

R. Muellenbach
Department of Anesthesiology, University Clinics of Wuerzburg

F. Schuster
Department of Anesthesiology, University Clinics of Wuerzburg

A. Koca
Department of Anesthesiology, University Clinics of Wuerzburg

C. Lintner
Department of Neurosurgery, University Clinics of Wuerzburg

E. Kunze
Department of Neurosurgery, University Clinics of Wuerzburg

J. Brederlau
Department of Anesthesiology, Clinics of Hanau

N. Roewer
Department of Anesthesiology, University Clinics of Wuerzburg

P. Steendijk
Laboratory of Cardiovascular Research, University of Leiden

C. Greim
Department of Anesthesiology, Clinics of Fulda